

The Hippo pathway terminal effector TAZ/WWTR1 mediates oxaliplatin sensitivity in colon cancer cells

Věra Slaninová, Lisa Heron-Milhavet, Mathilde Robin, Laura Jeanson, Diala Kantar, Diego Tosi, Laurent Bréhélin, Céline Gongora, Alexandre Djiane

▶ To cite this version:

Věra Slaninová, Lisa Heron-Milhavet, Mathilde Robin, Laura Jeanson, Diala Kantar, et al.. The Hippo pathway terminal effector TAZ/WWTR1 mediates oxaliplatin sensitivity in colon cancer cells. 2023. limm-04299945

HAL Id: lirmm-04299945 https://hal-lirmm.ccsd.cnrs.fr/lirmm-04299945v1

Preprint submitted on 22 Nov 2023

HAL is a multi-disciplinary open access archive for the deposit and dissemination of scientific research documents, whether they are published or not. The documents may come from teaching and research institutions in France or abroad, or from public or private research centers. L'archive ouverte pluridisciplinaire **HAL**, est destinée au dépôt et à la diffusion de documents scientifiques de niveau recherche, publiés ou non, émanant des établissements d'enseignement et de recherche français ou étrangers, des laboratoires publics ou privés.

1	The Hippo pathway terminal effector TAZ/WWTR1 mediates oxaliplatin sensitivity in
2	colon cancer cells
3	
4	
5	
6	Věra Slaninová ^{1#} , Lisa Heron-Milhavet ^{1#} , Mathilde Robin ^{1,2,3} , Laura Jeanson ¹ , Diala
7	Kantar ¹ , Diego Tosi ^{1,3} , Laurent Bréhélin ² , Céline Gongora ^{1*} , and Alexandre Djiane ^{1*}
8	
9	¹ IRCM, Univ Montpellier, Inserm, ICM, Montpellier, France
10	² LIRMM, Univ Montpellier, Inserm, CNRS, Montpellier, France
11	³ Fondazione Gianni Bonadonna, Milan, Italy
12	
13	*Authors for correspondence: IRCM, Inserm U1194
14	208, rue des Apothicaires
15	34298 Montpellier, Cedex, France
16	tel: +33 (0) 411 283 157
17	email: <u>alexandre.djiane@inserm.fr</u>
18	celine.gongora@inserm.fr
19	
20	# contributed equally
21	
22	KEY WORDS:
23	Oxaliplatin, colon cancer, Hippo signaling, TAZ, P53
24	

25 SUMMARY

26 YAP and TAZ, the Hippo pathway terminal transcriptional activators, are frequently 27 upregulated in cancers. In tumor cells, they have been mainly associated with increased 28 tumorigenesis controlling different aspects from cell cycle regulation, stemness, or resistance 29 to chemotherapies. In fewer cases, they have also been shown to oppose cancer progression, 30 including by promoting cell death through the action of the P73/YAP transcriptional complex, 31 in particular after chemotherapeutic drug exposure. Using several colorectal cancer cell lines, 32 we show here that oxaliplatin treatment led to a dramatic core Hippo pathway down-regulation 33 and nuclear accumulation of TAZ. We further show that TAZ was required for the increased 34 sensitivity of HCT116 cells to oxaliplatin, an effect that appeared independent of P73, but which required the nuclear relocalization of TAZ. Accordingly, Verteporfin and CA3, two 35 drugs affecting the activity of YAP and TAZ, showed an antagonistic with oxaliplatin in co-36 37 treatments. Our results support thus an early action of TAZ to sensitize cells to oxaliplatin, 38 consistent with a model in which nuclear TAZ in the context of DNA damage and P53 activity 39 pushes cells towards apoptosis. 40 41

42

43

44 INTRODUCTION

45 Colorectal cancer (CRC) is the third leading cause of cancer-related death worldwide 46 (Rawla et al., 2019). 30% of patients present synchronous metastases and 50-60% will develop 47 metastases that will require chemotherapy. The current management of advanced or metastatic 48 CRC is based on fluoropyrimidine (5-FU), oxaliplatin and irinotecan as single agents or more 49 often in combination (e.g. FOLFOX, FOLFIRI, or FOLFIRINOX; Xie et al., 2020). 50 Chemotherapy is combined with targeted therapy including monoclonal antibodies against 51 EGFR (e.g. cetuximab and panitumumab) or VEGF (bevacizumab), tyrosine kinase inhibitors 52 (e.g. regorafenib), and immune checkpoint blockade agents for patients with MSI-High tumors 53 (e.g. pembrolizumab; Xie et al., 2020).

54 Oxaliplatin is a third-generation platinum antitumor compound with a 1,2-diaminocyclohexane 55 (DACH) ligand (Chaney, 1995; Raymond et al., 1998). It induces mainly intra-strand 56 crosslinks, but also inter-strand crosslinks and DNA-protein crosslinks that stop DNA 57 replication and transcription, leading to apoptotic cell death (Perego and Robert, 2016; 58 Woynarowski et al., 2000, 1998). Oxaliplatin exerts its anti-tumor effect also by inducing 59 immunogenic cell death (Tesniere et al., 2010). Resistance to oxaliplatin can be either intrinsic 60 (primary resistance) or acquired (secondary resistance), and is usually tackled by combining 61 drugs to expose tumoral cells weaknesses or inhibit alternative survival pathways (Vasan et al., 62 2019). Despite intense research efforts in this field, more information on the molecular 63 mechanisms underlying oxaliplatin mechanism of action are needed to develop new treatment 64 strategies and improve the therapeutic response rate.

65 The Hippo signaling pathway represents an evolutionarily highly conserved growth control 66 pathway. First discovered through genetic screens in Drosophila, it consists of a central 67 cascade of core kinases: MST1/2 and LATS1/2 (homologues of *Drosophila* Hippo and Warts; 68 Heng et al., 2021; Pocaterra et al., 2020; Zheng and Pan, 2019). When activated, LATS1/2 69 phosphorylate YAP and WWTR1/TAZ (homologues of *Drosophila* Yki), two partly redundant 70 transcriptional co-activators which represent the terminal effector of the Hippo pathway 71 (Reggiani et al., 2021). Phosphorylated YAP and TAZ are retained in the cytoplasm through 72 binding to 14-3-3 proteins, and sent for proteasomal degradation. When the Hippo pathway is 73 not activated, hypo-phosphorylated YAP/TAZ enter the nucleus and bind to specific 74 transcription factors (TFs) to turn on the transcription of target genes. The best characterized 75 TF partners for YAP and TAZ are the TEADs (TEAD1-4, homologues of Drosophila 76 Scalloped; Heng et al., 2021; Pocaterra et al., 2020; Zheng and Pan, 2019). While depending 77 on cell type, the classic target genes include genes involved in proliferation, resistance to 78 apoptosis, cytoskeletal remodeling, or stemness (Rosenbluh et al., 2012; Tapon et al., 2002; 79 Totaro et al., 2018). But YAP/TAZ nucleo-cytoplasmic localization (and activity) is also 80 controlled by mechanical cues relayed by the actin cytoskeleton, or by cytoplasmic trapping 81 proteins such as AMOTs (Heng et al., 2021; Pocaterra et al., 2020; Zheng and Pan, 2019). 82 Importantly, the nuclear retention of YAP and TAZ is favored by tyrosine phosphorylation by 83 different kinases, and in particular SRC and YES (Byun et al., 2017; Ege et al., 2018; Li et al., 84 2016).

85 The Hippo pathway has been primarily described as a tumor suppressive pathway in a wide 86 variety of solid tumors (Kim and Kim, 2017; Li and Guan, 2022; Nguyen and Yi, 2019; 87 Thompson, 2020; Zheng and Pan, 2019) preventing the pro-tumoral effect of YAP/TAZ. 88 However, in CRCs the role of the Hippo pathway and of YAP and TAZ appears more complex. 89 Several studies point towards a classic pro-tumoral role for YAP and TAZ. In CRC patients 90 tumor samples, high expression and nuclear localizations of YAP correlated strongly with 91 disease evolution and bad prognosis (Ling et al., 2017; Steinhardt et al., 2008), or with 92 resistance to treatments such as 5FU or cetuximab (Kim and Kim, 2017; Lee et al., 2015; Touil 93 et al., 2014). Furthermore, invalidating YAP could blunt tumorigenic behaviors both in mice 94 CRC models (Shao et al., 2014) or in the metastatic HCT116 CRC cell line (Konsavage et al., 95 2012). However, YAP could exhibit a tumor suppressive role in CRCs. Studies in genetic 96 mouse models have shown that YAP/TAZ restricts canonical Wnt/β-Catenin signaling thus 97 preventing intestinal stem cells amplification, and could act as tumor suppressors in CRCs 98 (Azzolin et al., 2014, 2012; Barry et al., 2013). Similarly, the loss of core Hippo kinases 99 (LATS/MST) was recently shown to inhibit tumor progression in Apc mutant mouse models 100 and in patients-derived xenografts models (Cheung et al., 2020; Li et al., 2020).

101 The tumor suppressive role of YAP in CRC is further supported by its reported role in response 102 to DNA damage inducer drugs. Studies have shown that, in different cell lines including CRC 103 lines, cell death in response to cisplatin, doxorubicin, or etoposide, is mediated by P73, a 104 protein related to the tumor-suppressor P53. Following treatments, a YAP/P73 complex 105 accumulates in the nucleus, and triggers the transcription of P73 target genes involved in cell 106 death (Lapi et al., 2008; Strano et al., 2005, 2001). The direct interaction between YAP and 107 P73 is proposed to prevent P73 destabilization by the E3-Ubiquitin Ligase ITCH (Levy et al., 108 2007; Strano et al., 2005). This pro-apoptotic role of YAP is reminiscent to a similar role of 109 Yki in Drosophila (a Yki/p53 complex; Di Cara et al., 2015). Importantly, this appears specific to YAP, since TAZ cannot bind to P73, further suggesting that YAP and TAZ, while
performing redundant roles, also possess specific activities (Reggiani et al., 2021).

112 Given that oxaliplatin constitute one of the most used drugs in the treatment of CRCs, it is 113 important to evaluate its effects with respect to the Hippo pathway and to YAP/TAZ which can elicit conflicting roles to oppose or promote CRC tumorigenesis. We show here that upon 114 treatment with oxaliplatin, TAZ accumulated in the nucleus of CRC cell lines. We further show 115 116 that TAZ was required for early sensitivity of HCT116 to oxaliplatin. Interestingly, the nuclear localisation of TAZ was important, and drugs preventing this such as Dasatinib antagonized 117 118 the effect of oxaliplatin. These results support an early anti-tumoral role of YAP and TAZ in response to oxaliplatin suggesting particular attention to sequence of treatments and drug 119 120 combinations should be paid when considering potential future drugging of YAP/TAZ 121 signaling in the treatment of CRCs.

122

123 **RESULTS and DISCUSSION**

124 Oxaliplatin treatment triggers an early cell death program

125 Oxaliplatin is a third generation platinum compound widely used as part of the first line of 126 treatment for colon cancer patients in the FOLFOX regimen (Chaney, 1995; Raymond et al., 1998; Xie et al., 2020). Inside cells, oxaliplatin binds DNA, generating adducts which 127 128 ultimately lead to DNA breaks and replicative stress in proliferating cells. When used on 129 proliferating cancer cells, oxaliplatin treatment resulted in concentration-dependent cell death. 130 We measured the IC50 of oxaliplatin on HCT116 colon cancer cells at 0.5µM (Supplemental 131 Figure S1A). This dose reduced the amount of cells by 50% after 4 days of treatment. This 132 dose was about 10 fold lower than the oxaliplatin concentration reported in the blood of treated patients (between 3.7 and 7µM; Graham et al., 2000). The oxaliplatin dose used in this study 133 134 was thus compatible with the dose that could be ultimately found at the level of tumors in a 135 clinical setting, and did not represent an acute high concentration treatment, highlighting its 136 relevance for studying cellular responses to oxaliplatin. 137 When treated with oxaliplatin at IC50, HCT116 cells exhibited clear signs of DNA damage

such as accumulation of γH2AX, and 53BP1 puncta in the nuclei (Figure 1A&B). Consistently,
P53, which has been shown to control a specific cell death program in response to severe DNA

140 damage (for recent reviews Abuetabh et al., 2022; Panatta et al., 2021), accumulated strongly

141 24h after treatment (Figure 1C). Intriguingly, the P53 related protein P73, previously reported

142 to accumulate and to mediate cell death in response to DNA-damage inducing drugs such as

cisplatin, doxorubicin or etoposide, including in HCT116 cells (Lapi et al., 2008; Strano et al.,
2005), was destabilized upon oxaliplatin treatment. P63, the third member of the P53 protein

family, was not expressed in HCT116, even upon treatment (Figure 1C).

146 To better understand the cellular responses to oxaliplatin we profiled the changes in gene expression after 24h of exposure at IC 50. This analysis revealed that the expression of only a 147 148 limited number of genes were affected (fold change >1.5, adjusted p-value < 0.05): 253 upregulated and 111 down-regulated (Figure 1D; Supplemental Table 1). Gene ontology 149 150 enrichment approaches using the g:profiler online tool (Supplemental Table 2; Raudvere et al., 151 2019) highlighted that amongst the main cellular processes controlled by the upregulated genes 152 were DNA damage response (GO:0044819 mitotic G1/S transition checkpoint signaling; 153 GO:0000077 DNA damage checkpoint signaling...), apoptosis and cell death (GO:0045569 154 TRAIL binding; GO:0008219 cell death; GO:0012501 programmed cell death; GO:0006915 155 apoptotic process ...), and p53 response (GO:0072331 signal transduction by p53 class 156 mediator), consistent with the known role of oxaliplatin generating adducts on the DNA.

157 Indeed, many genes up-regulated have previously been associated with p53 signaling, and

158 represent p53 canonical target genes such as CDKN1A/P21, P53I3, BAX, or TIGAR

159 (REAC:R-HSA-3700989 Transcriptional Regulation by P53; WP:WP4963 p53 transcriptional

160 gene network). While up-regulated genes controlled mainly cell death programs, the down-

161 regulated genes were involved in DNA replication (GO:0006260) and cell cycle (GO:0007049)

162 consistent with the well documented effect of DNA damage on blocking cell cycle and

163 proliferation (Abuetabh et al., 2022).

Amongst the genes mis-regulated were also genes related to inflammation and immune cell recruitment (e.g. the upregulated genes CXCR2, EBI3/IL-27, or NLRP1, and the downregulated gene IL17RB) consistent with the previously reported role of oxaliplatin during immune cell death (Tesniere et al., 2010).

168 Finally, these analyses also highlighted several genes involved in cell architecture, namely 169 cytoskeleton and junctional complexes. Amongst the most striking features were changes in 170 the expression of integrin and extracellular matrix proteins engaging Integrins and Focal 171 Adhesions: collagens COL5A1 and COL12A1, as well as laminins LAMA3, LAMB3, and 172 LAMC1 and integrin ITGA3. These observations suggest that treated cells might remodel their 173 extracellular matrix, their Focal Adhesions, and the signaling pathways associated. The RNA-174 Seq analyses revealed also many changes to the cytoskeleton, including an upregulation of 175 several keratin-based intermediate filaments (KRT15/19/32) and associated factors (KRTAP2-176 3 and SFN). Several genes controlling the actin cytoskeleton were also affected such as the 177 branched actin regulators WDR63, CYFIP2, or WASF3, or different genes predicted to control 178 RHO activity (up: RHOD, EZR, and RAP2; down: ARHGAP18).

179

180 Taken together, these results suggest that upon oxaliplatin treatment, HCT116 cells implement 181 an early cell death program, which is likely mediated by the elevated P53 levels, and many 182 "bona-fide" P53 direct target genes involved in cell death are upregulated. Unlike other treatments such as cisplatin, doxorubicin, and etoposide (Lapi et al., 2008; Strano et al., 2005), 183 184 oxaliplatin is unlikely to mobilize the p73 anti-tumoral response since P73 levels are decreased 185 upon oxaliplatin treatment. The difference is striking when considering closely related 186 platinum compounds such as cisplatin and oxaliplatin. This difference is unlikely due to timing 187 as we could not observe any P73 up-regulation after oxaliplatin treatment even after shorter or 188 longer exposures. Even though dose comparisons between different compounds is tricky, we 189 note that the cisplatin dose was 50 times higher than that of oxaliplatin. Alternatively, while 190 both are thought to act primarily as generators of lethal amounts of DNA breaks, their 191 difference in mobilizing either P73 (cisplatin) or P53 (oxaliplatin) might arise from different 192

193

194 Oxaliplatin treatment triggers YAP and TAZ nuclear accumulation

alternative cellular effects independent of DNA damage.

195 Having established a regimen for treating HCT116 cells with oxaliplatin, and given the 196 complex reported roles of YAP/TAZ in CRCs (see Introduction), we investigated whether 197 YAP/TAZ could be affected, and thus monitored TEAD, YAP, and TAZ expressions and 198 localizations following oxaliplatin treatment.

199 After 24h (or 48h) of oxaliplatin treatment at the IC50, we did not observe any change in the 200 total levels or in the nuclear localization of TEAD4, the main TEAD paralogue in colon cells (Figure 2A). However, TAZ and YAP nuclear localizations increased following oxaliplatin 201 202 treatment in our culture conditions: the TAZ and YAP nuclear staining increased by 60% and 203 55% respectively when compared to untreated cells (Figure 2A). TAZ nuclear accumulation 204 was also observed in two other CRC cell lines: LoVo and Caco-2 (Supplemental Figure S2). 205 TAZ nuclear accumulation was further confirmed by fractionation experiments (Figure 2C; see 206 Materials and Methods). This increase in TAZ nuclear localization was reflected by an increase 207 in total TAZ levels by western blot analysis (Figure 2B). However, YAP total levels, and more 208 importantly the levels of YAP phosphorylation on Serine 127 (S127) were unchanged (Figure 209 2B).

210 The YAP S127 phosphorylation is deposited by the LATS1/2 Hippo pathway terminal kinases 211 and mediate the cytoplasmic retention of YAP by the 14-3-3 proteins and later targeting for proteasomal degradation (Heng et al., 2021; Pocaterra et al., 2020; Zheng and Pan, 2019). 212 213 Western-blot analyses on total protein extracts showed that several key proteins in the core 214 Hippo pathway were hypo-phosphorylated (p-MST1/2, p-MOB1) indicating a general lower 215 activity of the core Hippo pathway (Figure 2B). Total protein levels were also lower after 216 treatment, further suggesting a lower Hippo pathway activity in response to oxaliplatin, 217 consistent with the increased TAZ levels and increased nuclear TAZ localization (Figure 218 2A&C). However, given that levels of phospho-YAP and total YAP remained unchanged, how 219 the Hippo pathway down-regulation could have differing effects on YAP and TAZ remains to 220 be explored. YAP and TAZ appear only partly redundant, and YAP and TAZ specific 221 regulations have been reported (Reggiani et al., 2021). It is noteworthy that an additional 222 phospho-degron is present in TAZ, making it more sensitive to degradation than YAP. This 223 increased sensitivity might magnify TAZ level changes when the Hippo pathway is inhibited 224 by oxaliplatin (Azzolin et al., 2012). The decreased protein levels of different Hippo pathway 225 components in response to oxaliplatin were unlikely due to reduced mRNA abundance, since 226 we did not observe any change in our RNA-Seq, suggesting that it might be a consequence of 227 reduced translation and/or increased protein degradation. Indeed, previous studies have shown 228 that core Hippo pathway components can be regulated by ubiquitination such as LATS1 or 229 MOB1 (Ho et al., 2011; Lignitto et al., 2013; Salah et al., 2011). Whether oxaliplatin treatment 230 triggers a specific ubiquitin-mediated destabilization of the core Hippo pathway remains 231 however to be studied.

232

233 YAP is dispensable for Oxaliplatin-mediated cell death

234 Performing pathway analyses on the mis-regulated genes highlighted a strong activation of 235 p53 signaling (Supplemental Table S2). Motif enrichment analyses suggested that the p53 236 family of transcription factors were the main controllers of the up-regulated genes. With the exception of Axl, none of the "classic" YAP/TAZ target genes such as CTGF, CYR61/CCN1, 237 238 or BIRC2 (or genes involved in cell cycle progression, cytoskeleton regulation, or drug 239 resistance; (Pocaterra et al., 2020; Totaro et al., 2018) were up-regulated after oxaliplatin 240 treatment. We thus wondered what would be the role of YAP and TAZ in the response to 241 oxaliplatin treatment. Indeed, other anti-cancer drugs such as cisplatin have been shown to 242 promote cell death in part through the implementation of a P73/YAP-dependent cell death 243 program. Mechanistically, it has been proposed that DNA damage induced by cisplatin 244 stabilizes YAP which then binds and protects P73 from ITCH-mediated degradation (Levy et 245 al., 2007); the P73/YAP complex accumulates in the nucleus to turn on the expression of P73 target genes involved in cell death (Lapi et al., 2008; Strano et al., 2005, 2001). We thus 246 247 wondered whether the accumulation of TAZ (and the moderate accumulation of YAP) in the 248 nucleus could also participate in the cell death induced by oxaliplatin.

249 To test the requirement of YAP and TAZ, we invalidated YAP and TAZ by RNA interference. 250 The sole invalidation of YAP by shRNA led to a very modest reduction in oxaliplatin 251 sensitivity (IC50 in *shYAP* was determined at 0.62 compared to 0.52 in *shLuc* controls) (Figure 252 3A&C). It is noteworthy that, under the culture conditions used, YAP appeared dispensable for 253 HCT116 cells since the shRNA led to a knock-down efficiency >90%. These results suggest 254 that the cell death in response to oxaliplatin might not be dependent (or only marginally) on 255 the YAP/P73 complex as previously reported for other DNA-damage inducing compounds 256 (Lapi et al., 2008; Levy et al., 2007; Strano et al., 2005), but depends on alternative 257 mechanisms.

258

259 TAZ promotes cell death in response to oxaliplatin, independently of P73

260 We then investigated the role of TAZ. Strikingly, while the depletion of YAP had hardly 261 any effect, the combined knock-down of both YAP (shYAP) and TAZ (siTAZ), resulted in a 262 clear increase in resistance to oxaliplatin, where the IC50 reached 0.91µM in shYAP/siTAZ 263 HCT116 cells compared to 0.58µM in shLuc/siScrambled HCT116 control cells (Figure 264 3B&C), highlighting that TAZ participates to cell death in response to oxaliplatin. The effects 265 observed were specific to the *siTAZ*, since we observed a re-sensitization of treated cells when 266 complementing them with an expression vector for a murine version of *Taz* insensitive to the 267 siTAZ designed against human TAZ (Supplemental Figure S3A&B). We then wondered 268 whether the increased sensitivity promoted by TAZ could be dependent on P73, in a similar 269 mechanism as proposed for cisplatin. However, while P53 accumulated in response to 270 oxaliplatin in HCT116, P73 levels were decreased, undermining the role of P73 in response to this drug (Figure 1C). This absence of P73 stabilization, is consistent with the absence of 271 272 increased YAP levels after oxaliplatin treatment (Figure 2B). These results highlight that, 273 although overexpressed YAP could bind and stabilize endogenous P73 (Supplemental Figure 274 S4; Levy et al., 2007; Strano et al., 2005, 2001), oxaliplatin treatments at the clinically relevant 275 doses used, do not lead to YAP and P73 stabilization. We then confirmed that TAZ cannot bind 276 P73 (Supplemental Figure S4), ruling out that the elevated nuclear TAZ following oxaliplatin could act through a transcriptional complex with P73 to enhance cell death. A recent study 277 278 reported a direct interaction between TAZ and P53 in MCF7 and HCT116 cells, which resulted 279 in the inhibition of P53 activity towards senescence (Miyajima et al., 2020). However, when 280 we performed co-immunoprecipitation experiments, we were unable to document any 281 interaction between over-expressed YAP or overexpressed TAZ with endogenous P53 in 282 normal or oxaliplatin treated HCT116 cells (Supplemental Figure S4). Furthermore, the 283 increased oxaliplatin resistance of cells upon YAP/TAZ knockdown supports strongly that TAZ 284 acts to promote cell death and thus cooperates with P53 rather than antagonizes its activity as 285 suggested before (Miyajima et al., 2020). Taken together, these results suggest that the 286 sensitivity of HCT116 cells to oxaliplatin mediated by YAP and TAZ is not mediated by the 287 direct interaction of YAP or TAZ to P53 or P73.

288

289 Increased resistance to oxaliplatin upon YAP/TAZ activity blockade

290 The sh/siRNA interference results suggested that TAZ was required for sensitivity to 291 oxaliplatin. To validate independently the knock-down experiments, we used a 292 pharmacological approach with drugs targeting YAP/TAZ activity and monitored their action 293 in combination with oxaliplatin. We performed 2D matrices co-treatment analyses in which 294 cells were treated with increasing amounts of oxaliplatin and of the YAP/TAZ inhibitors 295 verteporfin or CA3 (Figure 3D and Supplemental Figure S1B &C; Liu-Chittenden et al., 2012; 296 Song et al., 2018). In both cases, the co-treatments led to a marked increase in the HCT116 297 resistance to oxaliplatin. Similar results were obtained on two other CRC cell lines: LoVo, and 298 Caco-2 (Supplemental Figure S3C&D). The mode of action of verteporfin remains unclear and 299 might involve increased retention in the cytoplasm of YAP and TAZ, or their degradation, 300 preventing them from complexing in the nucleus with their transcription factor partners (Wang 301 et al., 2016). A recent study showed that CA3 reduced the transcriptional activity mediated by 302 YAP/TAZ-TEAD (reduction in target genes expression), with only minor effects on YAP 303 protein levels (Morice et al., 2020). Even though the exact mode of action of verteporfin and 304 CA3 remain unclear, the increased resistance to oxaliplatin observed by co-treating cells with 305 YAP/TAZ pharmacological inhibitors, confirms the results obtained with the genetic knock-306 down, and supports a model where increased TAZ activity participate in the sensitivity of CRC 307 cells to oxaliplatin.

308

309 Src inhibition by Dasatinib reduces HCT116 cells sensitivity to oxaliplatin

310 The results suggest thus that preventing TAZ signaling in the early phases of oxaliplatin 311 treatment would represent a counter-productive approach, leading to reduced efficacy of 312 oxaliplatin to induce cell death. Besides the canonical Hippo signaling pathway, the nucleo-313 cytoplasmic shuttling of YAP and TAZ is under the control of many other inputs. In particular, 314 YAP and TAZ retention in the nucleus is promoted by the action of different tyrosine kinases, 315 such as ABL or SFKs (Src Family Kinases) which phosphorylate the C-termini of YAP and 316 TAZ (Y357 or Y316 respectively; Byun et al., 2017; Ege et al., 2018; Guégan et al., 2022; 317 Kedan et al., 2018; Lamar et al., 2019; Li et al., 2016). Due to its high relevance for colon 318 cancer, we focused our analysis on SRC, frequently activated in colon carcinoma (Sirvent et 319 al., 2020). An earlier study showed that depending on the colon cancer cell line considered, 320 SRC could be activated, inhibited, or not affected following oxaliplatin treatment (Kopetz et 321 al., 2009). We could replicate that SRC was not activated after 24h of oxaliplatin treatment in 322 HCT116 cells (as measured by phosphorylation on Y416; Figure 4A). Working with HCT116, 323 we are thus in a position to test the contribution of SRC to YAP/TAZ shuttling during 324 oxaliplatin treatment without the complications arising from treatment-induced acute SRC 325 activation. Previous reports suggested that the classic SRC kinase inhibitor Dasatinib could be

326 used as a drug to prevent YAP/TAZ signaling (Rosenbluh et al., 2012). Indeed, combining 327 Dasatinib with oxaliplatin treatment, prevented the nuclear accumulation of TAZ (Figure 4B). 328 The addition of Dasatinib to oxaliplatin treated cells led to a dramatic reduction of the TAZ 329 nuclear staining when compared to oxaliplatin alone (95% reduction; see Materials and 330 Methods). It should be noted however, that Dasatinib treatment at 50nM reduced slightly the 331 elevated global TAZ levels observed in response to oxaliplatin (Figure 4A). Nevertheless, even 332 though TAZ appeared a bit more unstable in presence of Dasatinib, its nucleo-cytoplasmic ratio was still profoundly affected by Dasatinib, preventing nuclear accumulation (Figure 4B). 333

- 334 We thus asked what would be the combined effect of Dasatinib treatment and oxaliplatin in 335 HCT116 cells. We thus performed 2D matrices co-treatment analyses in which cells were 336 treated with increasing amounts of oxaliplatin and of Dasatinib using drug ranges 337 encompassing their respective IC50 (0.5µM for oxaliplatin and 8µM for Dasatinib; 338 Supplemental Figure S1A&D). Strikingly combining both drugs showed clear regions of 339 antagonism, suggesting that Dasatinib treatment reduced HCT116 cells sensitivity to 340 oxaliplatin (Figure 4C). These results further support a model in which the nuclear 341 relocalization of TAZ in response to oxaliplatin treatment sensitizes cells, and caution the use 342 of Dasatinib in combination to oxaliplatin.
- 343

344 YAP/TAZ promote cell death in the early response to chemotherapeutic agents

Taken together the results presented here show that oxaliplatin promotes the fast nuclear relocalization of TAZ which then participates to the cells sensitivity to oxaliplatin. Given that we could not find any interaction between TAZ and P53 family members, but that the nuclear localization of TAZ is required for its effect, we could envision several models:

349 i) either the TAZ/TEAD transcription complex, in the context of DNA damage and P53

activation, promotes the transcription of specific early response genes promoting cell death;

351 ii) or the slight increase at the transcriptional level of "classic" YAP/TAZ/TEAD targets

352 involved in proliferation sensitizes cells to DNA damage and replicative stress;

iii) or alternatively, TAZ acts through a new complex involved in cell death, independently ofTEAD.

355 More studies should help to distinguish between these potential models.

356

357 YAP and TAZ, have been implicated in the resistance to various chemotherapies or targeted 358 therapies in different cancers (Kim and Kim, 2017; Nguyen and Yi, 2019; Zeng and Dong,

359 2021). It should be noted that the current study focuses on the immediate effects of oxaliplatin

within the first hours after exposure. Whether YAP and TAZ are later important for the 360 361 maintenance of the resistance acquired by the surviving clones is not addressed in this study. 362 Hints towards this later role of YAP/TAZ, are suggested by the elevated YAP levels reported 363 in many cancer cells following resistant clone selection (our own unpublished results, and (Kim 364 and Kim, 2017; Nguyen and Yi, 2019; Zeng and Dong, 2021). Functional studies impairing YAP demonstrated that YAP is indeed required for the tumorigenicity of resistant cells 365 366 (Yoshikawa et al., 2015). Furthermore, elevated YAP and TAZ nuclear staining is frequently 367 observed in patients tumor samples, including in CRCs (Li and Guan, 2022; Ling et al., 2017; 368 Steinhardt et al., 2008; Thompson, 2020). In advanced cancers, almost all patients undergo one 369 or more rounds of treatment before surgery, if surgery is possible. It is thus unclear whether 370 the increased YAP/TAZ nuclear levels observed in tumor samples reflect primary response to 371 treatment (as suggested by the current study), or whether they represent a secondary state that 372 might have been selected in the cells resistant to treatment.

The current study investigates the early response to oxaliplatin, supporting an early tumor 373 374 suppressive role of YAP/TAZ in response to treatment, in which, in the context of detrimental 375 DNA damage, YAP/TAZ activity promotes cell death. Is this role general or is it specific to 376 CRCs and oxaliplatin? Independently of the mechanism involved (YAP/P73 complex as 377 previously reported or alternative TAZ-mediated mechanisms as shown here), different breast 378 and colon cancer cell lines mobilize YAP or TAZ to promote cell death in response to many 379 different DNA damaging agents (Basu et al., 2003; Lapi et al., 2008; Levy et al., 2007; Strano 380 et al., 2005, 2001). This anti-tumoral role appears evolutionarily conserved and in Drosophila 381 the YAP/TAZ homologue Yki promotes cell death in response to different stress inducing agents (Di Cara et al., 2015), further suggesting that YAP/TAZ might promote cell death in 382 383 response to chemotherapeutic agents in other cancers beside CRCs and breast cancers. When 384 considering drugging YAP/TAZ signaling in the treatment of CRCs and other cancers, special 385 attention should thus be given to drug combinations, and importantly the sequence in which 386 they will be used.

387

388 MATERIALS AND METHODS

389 shRNA construction

- 390 shRNA directed against human YAP, TAZ, or the non-relevant Luciferase gene were designed
- 391 by adding to the selected targeted sequences, overhangs corresponding to BamHI and EcoRI
- 392 cloning sites at the 5'end of forward and reverse strand, respectively. Resulting oligos were
- 393 then annealed together and cloned into the pSIREN-RetroQ vector (TaKaRa) according to the
- 394 manufacturer's protocol between BamHI and EcoRI cloning sites.
- 395 Targeted sequences:
- 396 shRNA-YAP(3619): CAATCACTGTGTTGTATAT
- 397 *shRNA-TAZ(1417):* CCCTTTCTAACCTGGCTGT
- 398 shRNA-Luciferase: CGTACGCGGAATACTTCGA
- 399

400 Cell culture and cell transfections

- 401 Certified Human HCT 116 and LoVo colorectal cancer cell lines (RRID:CVCL_0291,
- 402 RRID:CVCL 0399) were obtained from LGC Standards (ATCC-CCL-247, ATCC-CCL-229).
- 403 Caco-2 cells (RRID:CVCL 0025) were certified independently. Cells were cultured in
- 404 RPMI1640 supplemented with 10% FBS at 37°C in a humidified atmosphere with 5% CO₂.
- 405 Cultures were regularly checked to be mycoplasma-free. No antibiotics were used to avoid any
- 406 cross-reaction with the Oxaliplatin treatment.
- 407 HCT116 cells expressing shRNA against YAP, TAZ, or Luciferase (Luc; control) were
- obtained by retroviral gene transduction of the corresponding pSIREN vectors. Retroviral
 particles were produced in HEK293 cells and subsequently used to infect HCT116 cells.
- 410 Positive clones were selected with $1 \mu g/mL$ puromycin and pooled together.
- 411 HCT116-shYAP/siTAZ cells were created by transfecting 100nM of TAZ siRNA (Dharmacon
- 412 siGENOME SMARTpool #M-016083-00-0005) into HCT116-shYAP cells using
- 413 Lipofectamine 2000 (Invitrogen) according to manufacturer's protocol. As a negative control,
- 414 100nM of *siScrambled* (D-001206-13) was transfected into HCT116-*shLuc* cells.
- 415 Murine Taz was expressed by transfecting cells with pEF-TAZ-N-Flag from Michael Yaffe
- 416 (Addgene #19025; RRID:Addgene_19025; Kanai et al., 2000).
- 417

418 **RNA-Seq**

419 HCT 116 cells were plated to reach 60 to 70% of confluence and treated with 0.5 μ M 420 Oxaliplatin (IC₅₀) for 24 hours. RNA was extracted using RNeasy plus mini kit (Qiagen),

- 421 quantified and analyzed for its integrity number (RIN) using a Bioanalyzer (Agilent 2100 at
- 422 the IRMB: https://irmb-montpellier.fr/single-service/transcriptome-ngs/). RNA (1 μ g) with
- 423 RIN between 8 and 10 were sent for RNA-Sequencing analysis to Fasteris biotechnology
- 424 company (http://www.fasteris.com). After library preparation, sequencing was performed on
- 425 the Illumina NovaSeq 6000 platform (S1 2x100 full FC). Mapping on the human genome
- 426 GRCh38 was performed using the protocol STAR 2.7.5b leading to 80-100 Millions reads per
- 427 condition. Normalization and pairwise differential expression analyses were performed using
- 428 the R package DESeq2 (2.13) (Anders and Huber, 2010).
- 429 RNA-Seq data has been deposited in NCBI's Gene Expression Omnibus under accession
- 430 number GSE227315.
- 431

432 Western blotting

- 433 Proteins issued from transfected untreated and treated HCT 116 cells were extracted, analyzed
- 434 by SDS-PAGE. Dilutions and antibodies' references are listed below.
- 435 Flag M2 (1/2000; Sigma-Aldrich #F1804)
- 436 GAPDH (1/3000; Proteintech #60004)
- 437 Histone H3 (1/1000; Cell Signaling Technology CST #4499)
- 438 LATS1 (1/1000; CST #3477)
- 439 MOB1 (1/1000; CST #13730)
- 440 p-MOB1 (1/1000; CST #8699)
- 441 MST1 (1/1000; CST #3682)
- 442 p-MST1/2 (1/1000; CST #49332)
- 443 NF2 antibody (Proteintech #26686-1-AP)
- 444 P53 (1/5000; Proteintech #10442-1-AP)
- 445 P63 (1/250; Santa Cruz #sc25268)
- 446 P73 (1/1000; CST #14620)
- 447 p-SRC Y416(1/1000; CST #2105)
- 448 TAZ (1/1000; CST #4883)
- 449 TEAD4 (1/250; Santa Cruz #sc101184)
- 450 Tubulin (1/10000; Sigma-Aldrich #T6074)
- 451 YAP (1/1000; CST #14074)
- 452 p-YAP S127 (1/1000; CST #13008)
- 453
- 454 Immunoprecipitation and co-immunoprecipitation

455 Protein extracts were prepared in lysis buffer (NaCl 150 mM, Tris pH 7.4 10 mM, EDTA 1 456 mM, Triton X-100 1%, NP-40 0.5%, cOmplete, EDTA-free protease inhibitors (Roche 457 #11873580001) for 30 min on ice before centrifugation. Immunoprecipitations were performed 458 overnight at 4°C on a rocking wheel using mouse EZview Red anti-Flag M2 affinity gel 459 (Sigma-Aldrich #F1804) after transfections of either p2xFlag CMV2 (empty vector), p2xFlag CMV2-YAP2 (YAP1; Addgene #19045) or p2xFlag CMV2-WWTR1 (TAZ). After Flag 460 461 immunoprecipitation, washes in lysis buffer were performed, followed by protein elution by 462 competition with 3XFLAG peptide (150 ng/µL final concentration) during 1 hour at 4°C. The 463 different immunoprecipitates were then subjected to Western blotting for detection of protein 464 complexes.

465

466 Immunofluorescence

467 Cells seeded on glass coverslips were fixed 10 min in paraformaldehyde (4 %), before being 468 permeabilized in PBS / 0.1% TritonX-100 for 10 min. After blocking in PBS / 0.5% BSA, cells 469 were incubated with primary antibodies overnight at 4C. Primary antibodies used are listed 470 below. Secondary Alexa Fluor Antibodies (1/600; Invitrogen) were used as described 471 previously (Kantar et al., 2021) for 1 hour at room temperature before mounting the coverslips 472 with Vectashield (Vector Laboratories #H-1200) and imaging on Zeiss Apotome or Leica 473 Thunder microscopes.

Antibodies used were rabbit anti-53BP1 (1/100; CST #4937), mouse anti-phospho-Histone
H2AX clone JBW301 (1/200; Millipore #05-636), anti-TAZ (1/100; CST #4883), mouse anti-

- 476 TEAD4 (1/50; Santa Cruz #sc101184), and rabbit anti-YAP (1/100; CST #14074).
- 477

478 Nuclear staining quantifications in HCT116 cells

479 Quantification was performed using ImageJ. Binary mask corresponding to the cell nuclei was 480 based on DAPI staining. Two nuclei touching each other (and therefore recognized as one on 481 binary mask) were manually separated by drawing a 2-pixel line between them. All incomplete 482 nuclei on the edge of the image as well as those that were in mitosis or mechanically damaged 483 were excluded from the analysis. The total signal was calculated as "corrected total cell 484 fluorescence" (CTCF) according to the following formula:

485 *CTCF* = Integrated Density – (Area of selected cell * Mean fluorescence of the background)

486 Background fluorescence was measured on three different spots (roughly the size of cell 487 nucleus) outside of the cell. In case of 53BP1 and g-H2AX staining, the whole area covered by

488 the nuclear mask was quantified as one. For YAP and TAZ nuclear staining, each cell was

quantified separately using particle analysis tool. Cytoplasmic levels of YAP and TAZ werenot quantified due to the small size of the cytoplasm in HCT116 cells.

491

492 *IC50 calculation and cytotoxicity*

493 Cell growth inhibition and cell viability after incubation with Oxaliplatin (Sigma Aldrich 494 #O9512), Verteporfin (Sigma Aldrich #SML0534), CA3 (CIL56, Selleckchem, #S8661) or 495 Dasatinib (Selleckchem #S1021) were assessed using the sulforhodamine B (SRB) assay. 496 Exponentially growing cells (750 cells/well) were seeded in 96-well plates in RPMI-1640 497 medium supplemented with 10% FCS. After 24 hours, serial dilutions of the tested drugs were 498 added and each concentration was tested in triplicate. After 96 hours, cells were fixed with 499 10% trichloroacetic acid and stained with 0.4% SRB in 1% acetic acid. SRB-fixed cells were 500 dissolved in 10 mmol/L Tris-HCl and absorbance at 540 nm was read using an MRX plate 501 reader (Dynex, Inc., Vienna, VA, USA). IC50 was determined graphically from the 502 cytotoxicity curves.

- For HCT116-*shYAP/siTAZ*, cells were transfected in 6 well plates 24h before starting the cell
 growth and cytotoxicity assays.
- 505

506 Quantification of the interaction effect

507 The interaction between the drugs tested *in vitro* was investigated with a concentration matrix 508 test, in which increasing concentration of each single drug were assessed with all possible 509 combinations of the other drugs. For each combination, the percentage of expected growing 510 cells in the case of effect independence was calculated according to the Bliss equation (Greco 511 et al., 1995):

512

$fu_c = fu_A fu_B$

where fu_c is the expected fraction of cells unaffected by the drug combination in the case of effect independence, and fu_A and fu_B are the fractions of cells unaffected by treatment *A* and *B*, respectively. The difference between the fu_c value and the fraction of living cells in the cytotoxicity test was considered as an estimation of the interaction effect, with positive values indicating synergism and negative values antagonism.

518 519

520 **REFERENCES**

- Abuetabh Y, Wu HH, Chai C, Al Yousef H, Persad S, Sergi CM, Leng R. 2022. DNA damage response
 revisited: the p53 family and its regulators provide endless cancer therapy opportunities.
 Exp Mol Med 54:1658–1669. doi:10.1038/s12276-022-00863-4
- 524Anders S, Huber W. 2010. Differential expression analysis for sequence count data. Genome Biol52511:R106. doi:10.1186/gb-2010-11-10-r106
- Azzolin L, Panciera T, Soligo S, Enzo E, Bicciato S, Dupont S, Bresolin S, Frasson C, Basso G, Guzzardo
 V, Fassina A, Cordenonsi M, Piccolo S. 2014. YAP/TAZ incorporation in the β-catenin
 destruction complex orchestrates the Wnt response. *Cell* 158:157–170.
 doi:10.1016/j.cell.2014.06.013
- Azzolin L, Zanconato F, Bresolin S, Forcato M, Basso G, Bicciato S, Cordenonsi M, Piccolo S. 2012.
 Role of TAZ as mediator of Wnt signaling. *Cell* 151:1443–1456.
 doi:10.1016/j.cell.2012.11.027
- Barry ER, Morikawa T, Butler BL, Shrestha K, de la Rosa R, Yan KS, Fuchs CS, Magness ST, Smits R,
 Ogino S, Kuo CJ, Camargo FD. 2013. Restriction of intestinal stem cell expansion and the
 regenerative response by YAP. *Nature* 493:106–110. doi:10.1038/nature11693
- Basu S, Totty NF, Irwin MS, Sudol M, Downward J. 2003. Akt phosphorylates the Yes-associated
 protein, YAP, to induce interaction with 14-3-3 and attenuation of p73-mediated apoptosis.
 Mol Cell 11:11–23. doi:10.1016/s1097-2765(02)00776-1
- Byun MR, Hwang J-H, Kim AR, Kim KM, Park JI, Oh HT, Hwang ES, Hong J-H. 2017. SRC activates TAZ
 for intestinal tumorigenesis and regeneration. *Cancer Lett* 410:32–40.
 doi:10.1016/j.canlet.2017.09.003
- 542Chaney S. 1995. The chemistry and biology of platinum complexes with the 1,2-diaminocyclohexane543carrier ligand (review). Int J Oncol 6:1291–1305. doi:10.3892/ijo.6.6.1291
- 544 Cheung P, Xiol J, Dill MT, Yuan W-C, Panero R, Roper J, Osorio FG, Maglic D, Li Q, Gurung B, Calogero
 545 RA, Yilmaz ÖH, Mao J, Camargo FD. 2020. Regenerative Reprogramming of the Intestinal
 546 Stem Cell State via Hippo Signaling Suppresses Metastatic Colorectal Cancer. *Cell Stem Cell* 547 27:590-604.e9. doi:10.1016/j.stem.2020.07.003
- 548 Di Cara F, Maile TM, Parsons BD, Magico A, Basu S, Tapon N, King-Jones K. 2015. The Hippo pathway
 549 promotes cell survival in response to chemical stress. *Cell Death Differ* 22:1526–1539.
 550 doi:10.1038/cdd.2015.10
- Ege N, Dowbaj AM, Jiang M, Howell M, Hooper S, Foster C, Jenkins RP, Sahai E. 2018. Quantitative
 Analysis Reveals that Actin and Src-Family Kinases Regulate Nuclear YAP1 and Its Export. *Cell Syst* 6:692-708.e13. doi:10.1016/j.cels.2018.05.006
- 554Graham MA, Lockwood GF, Greenslade D, Brienza S, Bayssas M, Gamelin E. 2000. Clinical555pharmacokinetics of oxaliplatin: a critical review. Clin Cancer Res 6:1205–1218.
- 556Greco WR, Bravo G, Parsons JC. 1995. The search for synergy: a critical review from a response557surface perspective. Pharmacol Rev 47:331–385.
- Guégan J-P, Lapouge M, Voisin L, Saba-El-Leil MK, Tanguay P-L, Lévesque K, Brégeon J, Mes-Masson
 A-M, Lamarre D, Haibe-Kains B, Trinh VQ, Soucy G, Bilodeau M, Meloche S. 2022. Signaling
 by the tyrosine kinase Yes promotes liver cancer development. *Sci Signal* 15:eabj4743.
 doi:10.1126/scisignal.abj4743
- Heng BC, Zhang X, Aubel D, Bai Y, Li X, Wei Y, Fussenegger M, Deng X. 2021. An overview of signaling
 pathways regulating YAP/TAZ activity. *Cell Mol Life Sci* 78:497–512. doi:10.1007/s00018-020 03579-8
- Ho KC, Zhou Z, She Y-M, Chun A, Cyr TD, Yang X. 2011. Itch E3 ubiquitin ligase regulates large tumor
 suppressor 1 stability [corrected]. *Proc Natl Acad Sci U S A* 108:4870–4875.
 doi:10.1073/pnas.1101273108
- Kanai F, Marignani PA, Sarbassova D, Yagi R, Hall RA, Donowitz M, Hisaminato A, Fujiwara T, Ito Y,
 Cantley LC, Yaffe MB. 2000. TAZ: a novel transcriptional co-activator regulated by

570	interactions with 14-3-3 and PDZ domain proteins. <i>EMBO J</i> 19 :6778–6791.
571	doi:10.1093/emboj/19.24.6778
572	Kantar D, Mur EB, Mancini M, Slaninova V, Salah YB, Costa L, Forest E, Lassus P, Géminard C,
573	Boissière-Michot F, Orsetti B, Theillet C, Colinge J, Benistant C, Maraver A, Heron-Milhavet L,
574	Djiane A. 2021. MAGI1 inhibits the AMOTL2/p38 stress pathway and prevents luminal breast
575	tumorigenesis. <i>Sci Rep</i> 11 :5752. doi:10.1038/s41598-021-85056-1
576	Kedan A, Verma N, Saroha A, Shreberk-Shaked M, Müller A-K, Nair NU, Lev S. 2018. PYK2 negatively
577	regulates the Hippo pathway in TNBC by stabilizing TAZ protein. <i>Cell Death Dis</i> 9 :985.
578	doi:10.1038/s41419-018-1005-z
579	Kim MH, Kim J. 2017. Role of YAP/TAZ transcriptional regulators in resistance to anti-cancer
580	therapies. Cell Mol Life Sci 74:1457–1474. doi:10.1007/s00018-016-2412-x
581	Konsavage WM, Kyler SL, Rennoll SA, Jin G, Yochum GS. 2012. Wnt/β-catenin signaling regulates Yes-
582	associated protein (YAP) gene expression in colorectal carcinoma cells. J Biol Chem
583	287 :11730–11739. doi:10.1074/jbc.M111.327767
584	Kopetz S, Lesslie DP, Dallas NA, Park SI, Johnson M, Parikh NU, Kim MP, Abbruzzese JL, Ellis LM,
585	Chandra J, Gallick GE. 2009. Synergistic activity of the SRC family kinase inhibitor dasatinib
586	and oxaliplatin in colon carcinoma cells is mediated by oxidative stress. <i>Cancer Res</i> 69:3842–
587	3849. doi:10.1158/0008-5472.CAN-08-2246
588	Lamar JM, Xiao Y, Norton E, Jiang Z-G, Gerhard GM, Kooner S, Warren JSA, Hynes RO. 2019. SRC
589	tyrosine kinase activates the YAP/TAZ axis and thereby drives tumor growth and metastasis.
590	<i>J Biol Chem</i> 294 :2302–2317. doi:10.1074/jbc.RA118.004364
591	Lapi E, Di Agostino S, Donzelli S, Gal H, Domany E, Rechavi G, Pandolfi PP, Givol D, Strano S, Lu X,
592	Blandino G. 2008. PML, YAP, and p73 are components of a proapoptotic autoregulatory
593	feedback loop. <i>Mol Cell</i> 32 :803–814. doi:10.1016/j.molcel.2008.11.019
594	Lee K-W, Lee SS, Kim S-B, Sohn BH, Lee H-S, Jang H-J, Park Y-Y, Kopetz S, Kim SS, Oh SC, Lee J-S. 2015.
595	Significant association of oncogene YAP1 with poor prognosis and cetuximab resistance in
596	colorectal cancer patients. <i>Clin Cancer Res</i> 21 :357–364. doi:10.1158/1078-0432.CCR-14-
597	
598	Levy D, Adamovich Y, Reuven N, Shaul Y. 2007. The Yes-associated protein 1 stabilizes p73 by
599 600	preventing Itch-mediated ubiquitination of p73. <i>Cell Death Differ</i> 14 :743–751.
600 601	doi:10.1038/sj.cdd.4402063
601 602	Li F-L, Guan K-L. 2022. The two sides of Hippo pathway in cancer. <i>Semin Cancer Biol</i> 85 :33–42.
602 603	doi:10.1016/j.semcancer.2021.07.006
603 604	Li P, Silvis MR, Honaker Y, Lien W-H, Arron ST, Vasioukhin V. 2016. αE-catenin inhibits a Src-YAP1
604 605	oncogenic module that couples tyrosine kinases and the effector of Hippo signaling pathway. <i>Genes Dev</i> 30 :798–811. doi:10.1101/gad.274951.115
606	Li Q, Sun Y, Jarugumilli GK, Liu S, Dang K, Cotton JL, Xiol J, Chan PY, DeRan M, Ma L, Li R, Zhu LJ, Li JH,
607	Leiter AB, Ip YT, Camargo FD, Luo X, Johnson RL, Wu X, Mao J. 2020. Lats1/2 Sustain
608	Intestinal Stem Cells and Wnt Activation through TEAD-Dependent and Independent
609	Transcription. <i>Cell Stem Cell</i> 26 :675-692.e8. doi:10.1016/j.stem.2020.03.002
610	Lignitto L, Arcella A, Sepe M, Rinaldi L, Delle Donne R, Gallo A, Stefan E, Bachmann VA, Oliva MA,
611	Tiziana Storlazzi C, L'Abbate A, Brunetti A, Gargiulo S, Gramanzini M, Insabato L, Garbi C,
612	Gottesman ME, Feliciello A. 2013. Proteolysis of MOB1 by the ubiquitin ligase praja2
613	attenuates Hippo signalling and supports glioblastoma growth. Nat Commun 4 :1822.
614	doi:10.1038/ncomms2791
615	Ling H-H, Kuo C-C, Lin B-X, Huang Y-H, Lin C-W. 2017. Elevation of YAP promotes the epithelial-
616	mesenchymal transition and tumor aggressiveness in colorectal cancer. <i>Exp Cell Res</i>
617	350 :218–225. doi:10.1016/j.yexcr.2016.11.024
618	Liu-Chittenden Y, Huang B, Shim JS, Chen Q, Lee S-J, Anders RA, Liu JO, Pan D. 2012. Genetic and
619	pharmacological disruption of the TEAD-YAP complex suppresses the oncogenic activity of
620	YAP. Genes Dev 26 :1300–1305. doi:10.1101/gad.192856.112
020	

Miyajima C, Kawarada Y, Inoue Y, Suzuki C, Mitamura K, Morishita D, Ohoka N, Imamura T, Hayashi

621

622 H. 2020. Transcriptional Coactivator TAZ Negatively Regulates Tumor Suppressor p53 623 Activity and Cellular Senescence. Cells 9:171. doi:10.3390/cells9010171 624 Morice S, Mullard M, Brion R, Dupuy M, Renault S, Tesfaye R, Brounais-Le Royer B, Ory B, Redini F, 625 Verrecchia F. 2020. The YAP/TEAD Axis as a New Therapeutic Target in Osteosarcoma: Effect 626 of Verteporfin and CA3 on Primary Tumor Growth. Cancers (Basel) 12:3847. 627 doi:10.3390/cancers12123847 628 Nguyen CDK, Yi C. 2019. YAP/TAZ Signaling and Resistance to Cancer Therapy. Trends Cancer 5:283– 629 296. doi:10.1016/j.trecan.2019.02.010 630 Panatta E, Zampieri C, Melino G, Amelio I. 2021. Understanding p53 tumour suppressor network. 631 Biol Direct 16:14. doi:10.1186/s13062-021-00298-3 632 Perego P, Robert J. 2016. Oxaliplatin in the era of personalized medicine: from mechanistic studies 633 to clinical efficacy. Cancer Chemother Pharmacol 77:5–18. doi:10.1007/s00280-015-2901-x 634 Pocaterra A, Romani P, Dupont S. 2020. YAP/TAZ functions and their regulation at a glance. J Cell Sci 635 133:jcs230425. doi:10.1242/jcs.230425 636 Raudvere U, Kolberg L, Kuzmin I, Arak T, Adler P, Peterson H, Vilo J. 2019. g:Profiler: a web server for 637 functional enrichment analysis and conversions of gene lists (2019 update). Nucleic Acids Res 638 47:W191–W198. doi:10.1093/nar/gkz369 639 Rawla P, Sunkara T, Barsouk A. 2019. Epidemiology of colorectal cancer: incidence, mortality, 640 survival, and risk factors. Prz Gastroenterol 14:89–103. doi:10.5114/pg.2018.81072 641 Raymond E, Faivre S, Woynarowski JM, Chaney SG. 1998. Oxaliplatin: mechanism of action and 642 antineoplastic activity. Semin Oncol 25:4–12. 643 Reggiani F, Gobbi G, Ciarrocchi A, Sancisi V. 2021. YAP and TAZ Are Not Identical Twins. Trends 644 Biochem Sci 46:154–168. doi:10.1016/j.tibs.2020.08.012 645 Rosenbluh J, Nijhawan D, Cox AG, Li X, Neal JT, Schafer EJ, Zack TI, Wang X, Tsherniak A, Schinzel AC, 646 Shao DD, Schumacher SE, Weir BA, Vazquez F, Cowley GS, Root DE, Mesirov JP, Beroukhim R, 647 Kuo CJ, Goessling W, Hahn WC. 2012. β-Catenin-driven cancers require a YAP1 648 transcriptional complex for survival and tumorigenesis. Cell 151:1457–1473. 649 doi:10.1016/j.cell.2012.11.026 650 Salah Z, Melino G, Ageilan RI. 2011. Negative regulation of the Hippo pathway by E3 ubiquitin ligase 651 ITCH is sufficient to promote tumorigenicity. *Cancer Res* **71**:2010–2020. doi:10.1158/0008-652 5472.CAN-10-3516 653 Shao DD, Xue W, Krall EB, Bhutkar A, Piccioni F, Wang X, Schinzel AC, Sood S, Rosenbluh J, Kim JW, 654 Zwang Y, Roberts TM, Root DE, Jacks T, Hahn WC. 2014. KRAS and YAP1 converge to regulate 655 EMT and tumor survival. Cell 158:171–184. doi:10.1016/j.cell.2014.06.004 656 Sirvent A, Mevizou R, Naim D, Lafitte M, Roche S. 2020. Src Family Tyrosine Kinases in Intestinal 657 Homeostasis, Regeneration and Tumorigenesis. Cancers (Basel) 12:E2014. 658 doi:10.3390/cancers12082014 659 Song S, Xie M, Scott AW, Jin J, Ma L, Dong X, Skinner HD, Johnson RL, Ding S, Ajani JA. 2018. A Novel 660 YAP1 Inhibitor Targets CSC-Enriched Radiation-Resistant Cells and Exerts Strong Antitumor 661 Activity in Esophageal Adenocarcinoma. Mol Cancer Ther 17:443–454. doi:10.1158/1535-662 7163.MCT-17-0560 663 Steinhardt AA, Gayyed MF, Klein AP, Dong J, Maitra A, Pan D, Montgomery EA, Anders RA. 2008. 664 Expression of Yes-associated protein in common solid tumors. Hum Pathol 39:1582–1589. 665 doi:10.1016/j.humpath.2008.04.012 666 Strano S, Monti O, Pediconi N, Baccarini A, Fontemaggi G, Lapi E, Mantovani F, Damalas A, Citro G, 667 Sacchi A, Del Sal G, Levrero M, Blandino G. 2005. The transcriptional coactivator Yes-668 associated protein drives p73 gene-target specificity in response to DNA Damage. Mol Cell 669 18:447-459. doi:10.1016/j.molcel.2005.04.008

Strano S, Munarriz E, Rossi M, Castagnoli L, Shaul Y, Sacchi A, Oren M, Sudol M, Cesareni G, Blandino

670

671 G. 2001. Physical interaction with Yes-associated protein enhances p73 transcriptional 672 activity. J Biol Chem 276:15164-15173. doi:10.1074/jbc.M010484200 673 Tapon N, Harvey KF, Bell DW, Wahrer DCR, Schiripo TA, Haber DA, Hariharan IK. 2002. salvador 674 Promotes both cell cycle exit and apoptosis in Drosophila and is mutated in human cancer 675 cell lines. Cell 110:467-478. doi:10.1016/s0092-8674(02)00824-3 676 Tesniere A, Schlemmer F, Boige V, Kepp O, Martins I, Ghiringhelli F, Aymeric L, Michaud M, Apetoh L, 677 Barault L, Mendiboure J, Pignon J-P, Jooste V, van Endert P, Ducreux M, Zitvogel L, Piard F, 678 Kroemer G. 2010. Immunogenic death of colon cancer cells treated with oxaliplatin. 679 Oncogene 29:482-491. doi:10.1038/onc.2009.356 680 Thompson BJ. 2020. YAP/TAZ: Drivers of Tumor Growth, Metastasis, and Resistance to Therapy. 681 Bioessays 42:e1900162. doi:10.1002/bies.201900162 682 Totaro A, Panciera T, Piccolo S. 2018. YAP/TAZ upstream signals and downstream responses. Nat Cell 683 Biol 20:888-899. doi:10.1038/s41556-018-0142-z 684 Touil Y, Igoudjil W, Corvaisier M, Dessein A-F, Vandomme J, Monté D, Stechly L, Skrypek N, Langlois 685 C, Grard G, Millet G, Leteurtre E, Dumont P, Truant S, Pruvot F-R, Hebbar M, Fan F, Ellis LM, 686 Formstecher P, Van Seuningen I, Gespach C, Polakowska R, Huet G. 2014. Colon cancer cells 687 escape 5FU chemotherapy-induced cell death by entering stemness and quiescence 688 associated with the c-Yes/YAP axis. Clin Cancer Res 20:837-846. doi:10.1158/1078-689 0432.CCR-13-1854 690 Vasan N, Baselga J, Hyman DM. 2019. A view on drug resistance in cancer. *Nature* 575:299–309. 691 doi:10.1038/s41586-019-1730-1 692 Wang C, Zhu X, Feng W, Yu Y, Jeong K, Guo W, Lu Y, Mills GB. 2016. Verteporfin inhibits YAP function 693 through up-regulating 14-3-3σ sequestering YAP in the cytoplasm. Am J Cancer Res 6:27–37. 694 Woynarowski JM, Chapman WG, Napier C, Herzig MC, Juniewicz P. 1998. Sequence- and region-695 specificity of oxaliplatin adducts in naked and cellular DNA. Mol Pharmacol 54:770–777. 696 doi:10.1124/mol.54.5.770 697 Woynarowski JM, Faivre S, Herzig MC, Arnett B, Chapman WG, Trevino AV, Raymond E, Chaney SG, 698 Vaisman A, Varchenko M, Juniewicz PE. 2000. Oxaliplatin-induced damage of cellular DNA. 699 Mol Pharmacol 58:920-927. doi:10.1124/mol.58.5.920 700 Xie Y-H, Chen Y-X, Fang J-Y. 2020. Comprehensive review of targeted therapy for colorectal cancer. 701 *Signal Transduct Target Ther* **5**:22. doi:10.1038/s41392-020-0116-z 702 Yoshikawa K, Noguchi K, Nakano Y, Yamamura M, Takaoka K, Hashimoto-Tamaoki T, Kishimoto H. 703 2015. The Hippo pathway transcriptional co-activator, YAP, confers resistance to cisplatin in 704 human oral squamous cell carcinoma. Int J Oncol 46:2364–2370. doi:10.3892/ijo.2015.2948 705 Zeng R, Dong J. 2021. The Hippo Signaling Pathway in Drug Resistance in Cancer. Cancers (Basel) 706 13:318. doi:10.3390/cancers13020318 707 Zheng Y, Pan D. 2019. The Hippo Signaling Pathway in Development and Disease. Dev Cell 50:264-708 282. doi:10.1016/j.devcel.2019.06.003 709 710 711

712 ACKNOWLEDGEMENTS

713 The authors thank the different lab members of the Djiane and Gongora teams for helpful 714 discussions. VS was supported by Fondation de France. MR was supported by LabEx 715 NUMEV. DK was supported by Ligue Contre le Cancer. This work was supported by grants 716 from Fondation ARC (#PJA 20141201630) and Ligue Nationale Contre le Cancer (Région 717 Languedoc-Roussillon) to LHM and AD. Work in the lab of CG was also supported by grants 718 and funds from INSERM, the Institut du cancer de Montpellier (ICM), SIRIC (SIRIC 719 Montpellier Cancer Grant «INCa-DGOS-Inserm 6045»), Cancéropole GSO, and the program 720 «investissement d'avenir» (grant agreement: Labex MabImprove, ANR-10-LABX-53-01). 721 722 723 **AUTHOR CONTRIBUTIONS** 724 VS, LHM, LJ, and DK performed experiments. CG and AD designed the experiments. VS, LHM, MR, DK, CG and AD analyzed the data. VS, LHM, DT, LB, CG, and AD interpreted 725 726 the data. CG and AD wrote the manuscript. 727 728 729 **COMPETING INTERESTS** 730 All authors declare no competing interest 731

732 FIGURE LEGENDS

733 Figure 1. Oxaliplatin treatment induces DNA damage

- A. Immunofluorescence experiments performed on HCT116 cells treated, or not, with
- oxaliplatin (0.5 μ M) monitoring γ -H2AX (yellow). DAPI (blue) was used to stain DNA and
- the nuclei. Quantification of the staining is shown on the right side and is represented as the
- 737 corrected nuclear fluorescence. Data are represented as the mean \pm SEM. (n=3). Unpaired two-
- 738 tailed Student's t-test; ** p<0.01.
- 739 B. Immunofluorescence experiments performed on HCT116 cells treated, or not, with
- 740 oxaliplatin (0.5 μM) monitoring 53BP1 (grey). DAPI (blue) was used to stain DNA and the
- 741 nuclei. Quantification of the staining is shown on the right side and is represented as the
- 742 corrected nuclear fluorescence. Data are represented as the mean \pm SEM. (n=3). Unpaired two-
- 743 tailed Student's t-test; *** p<0.001.
- 744 C. Western blot analysis showing protein expression of TEAD4 and p53 family of proteins in
- HCT116 treated (Oxa), or not (NT) with oxaliplatin (0.5 μ M). GAPDH was used as a loading control (n=3).
- D. Heat map corresponding to the genes differentially expressed in HCT116 cells after 24h of
 oxaliplatin treatment at IC50 (see Supplemental Table 1). The three replicates for the nontreated (NT) and treated (Oxa) are shown.
- 750

751 Figure 2. Oxaliplatin treatment triggers YAP and TAZ nuclear accumulation

- A. Immunofluorescence experiments performed on HCT116 cells treated, or not, with oxaliplatin (0.5 μ M) monitoring TEAD4 (top panels), YAP (middle panels), and TAZ (bottom panels) nuclear localization (red). DAPI (blue) was used to stain DNA and the nuclei. Quantification of both stainings are shown on the right side of the figures and are represented as the corrected nuclear fluorescence. Data are represented as the mean ± SEM (n=3). Unpaired two-tailed Student's t-test; **** p < 0.0001.
- **B.** Western blot analysis showing protein expression and/or activation of Hippo pathway components in HCT116 cells treated (Oxa), or not (NT) with oxaliplatin (0.5 μ M). GAPDH was used as a loading control (n=3).
- 761 C. Western blot analysis after subcellular fractionation showing the relative amount of YAP
- and TAZ protein in the nuclear fraction of HCT116 cells treated (Oxa), or not (NT) with
- 763 oxaliplatin (0.5 μ M). Histone H3 was used as a nuclear loading control for the fractionation
- 764 (n=3).

765

766 Figure 3. YAP and TAZ are required for oxaliplatin-mediated cell death

A. HCT116-shYAP and HCT116-shLuc cell lines were treated with increasing doses of
 oxaliplatin for 96h. Cell viability analysis was then assessed using SRB assay and the IC50 of

oxaliplatin was calculated as the concentration needed to kill 50% of the cells (shown in the inset). Paired two-tailed Student's t-test ,* p<0.05.

- 771 B. HCT116-shYAP-siTAZ and HCT116-shLuc-siCtl (control) cell lines were treated with
- increasing doses of oxaliplatin for 96h. Cell viability analysis was then assessed using SRB
- assay and the IC50 of oxaliplatin was calculated as the concentration needed to kill 50% of the
- cells (shown in the inset). Paired two-tailed Student's t-test, ** p<0.01.
- 775 C. Western blot analysis showing protein expression of TAZ and YAP in HCT116-shLuc, -

siTAZ, *-shYAP* and both *-shYAP-siTAZ* used in panel A and B. Tubulin was used as a loading
control (n=3).

778 D. HCT116 cells were incubated with increasing concentrations of oxaliplatin and either

Verteporfin or CA3. Cell viability was assessed with the SRB assay in 2D to obtain the viability
 matrix. Drug concentrations were as follows: Verteporfin (from 0.437 to 7 µM), CA3 (from

781 0.004 to 0.75 μ M) and Oxaliplatin (from 0.0185 to 1.2 μ M). The synergy matrices were

- 782 calculated as described in Materials and Methods.
- 783

784 Figure 4. Src inhibition by Dasatinib reduces HCT116 cells sensitivity to oxaliplatin

A. Western blot analysis showing protein expression of YAP and TAZ in HCT116 treated, or not, with oxaliplatin (0.5 μ M) and/or Dasatinib (50 nM and 100 nM). Phopsho-SRC blotting was used to evaluate the inhibition of SRC activity using Dasatinib. GAPDH was used as a loading control (n=3). Quantification of the blots (performed using Image J software) is shown on the right side of the figure.

B. Immunofluorescence experiments performed in HCT116 cells treated, or not, with oxaliplatin (0.5 μ M) and/or Dasatinib (50 nM) monitoring YAP (top panels) and TAZ (bottom panels) nuclear localization (red). DAPI (blue) was used to stain DNA and the nuclei. Quantification of both stainings are shown on the right side of the figures and are represented as the corrected nuclear fluorescence. Data are represented as the mean ± SEM (n=3). Unpaired two-tailed Student's t-test; ****p < 0.0001.

796 C. HCT116 colorectal cancer cell lines were incubated with increasing concentrations of 797 oxaliplatin and Dasatinib. Cell viability was assessed with the SRB assay in 2D to obtain the 798 viability matrix. Drug concentrations were as follows: Dasatinib (from 1 to 16 μ M) and 799 oxaliplatin (from 0.0185 to 1.2 µM). The synergy matrix was calculated as described in 800 Materials and Methods. 801 802 803 804 SUPPLEMENTAL FIGURE LEGENDS 805 806 Supplemental Figure S1. Cell viability in response to drugs 807 Cells were treated with increasing doses of oxaliplatin (A), Verteporfin (B), CA3 (C) and 808 Dasatinib (D) for 96h. Cell viability analysis was then assessed using SRB assay and the IC50 809 of each drug could be calculated as the concentration that reduced cell numbers by 50% (shown 810 in the insets). 811 Supplemental Figure S2. TAZ nuclear accumulation in LoVo and Caco-2 CRC cell lines 812 813 A-B. Immunofluorescence experiments performed on LoVo (A) and Caco-2 (B) cells treated 814 or not, with oxaliplatin at IC50 (0.6 μ M and 0.3 μ M respectively) monitoring TAZ nuclear 815 localization (green). DAPI (blue) was used to stain DNA and the nuclei. Quantifications are 816 shown on the right side of the figure and are represented as the corrected nuclear fluorescence. 817 Data are represented as the mean \pm SEM. Unpaired two-tailed Student's t-test; **** p < 0.0001. 818 819 Supplemental Figure S3. TAZ mediates sensitivity to oxaliplatin in CRC cell lines 820 A. HCT116-shYAP-siScramb (control), HCT116-shYAP-siTAZ, and HCT116-shYAP-siTAZ transfected with a Flag tagged murine Taz (*pEFmTaz*) cell lines were treated with increasing 821 822 doses of oxaliplatin for 96h. Cell viability analysis was then assessed using SRB assay and the 823 IC50 of oxaliplatin was calculated as the concentration needed to kill 50% of the cells. Paired 824 two-tailed Student's t-test, ** p<0.01, ns non-significant. 825 **B**. Western blot analysis showing protein expression of TAZ and Flag in the different cell lines 826 used in panel A. GAPDH was used as a loading control. C-D. LoVo (C) and Caco-2 (D) cells were incubated with increasing concentrations of 827 828 oxaliplatin and either Verteporfin or CA3. Cell viability was assessed with the SRB assay in 829 2D to obtain the viability matrix. Drug concentrations were as follows: Verteporfin (from 0.875 830 to 14 μ M), CA3 (from 0.15 to 2.4 μ M) and Oxaliplatin (from 0.075 to 4.8 μ M). The synergy 831 matrices were calculated as described in Materials and Methods. 832

833	Supplemental Figure S4. Interaction between YAP/TAZ and P53 protein family members
834	in HCT116 cells
835	Western blot analysis of Flag (YAP or TAZ) immunoprecipitates on protein extracts from
836	HCT116 treated (Oxa), or not (NT) showing an interaction between YAP and p73 (n=3).
837	
838	
839	Supplemental Table 1. Differentially expressed genes in HCT116 cells after oxaliplatin
840	treatment for 24h at IC50
841	Only differentially expressed genes with an adjusted p-value< 0.05 are shown. Columns are:
842	test_id: position and description of the feature tested
843	ENSG_ID: Ensemble gene ID
844	symbol: gene symbol
845	sample_1: first group in the comparison; untreated cells
846	sample_2: second group in the comparison; cells treated with oxaliplatin
847	mean_1: mean of normalized count for the first group in the comparison
848	mean_2: mean of normalized count for the second group in the comparison
849	log2FoldChange: log2 fold change estimates
850	pvalue: pvalue
851	padj: pvalue adjusted for multiple testing with the Benjamini-Hochberg procedure, which
852	controls false discovery rate (FDR)
853	
854	Supplemental Table 2. g:profiler functional enrichment analyses
855	Columns are :
856	GO_ID: Gene Ontology
857	KEGG_ID: KEGG pathways
858	REAC_ID: Reactome pathways
859	WP_ID: WikiPathways
860	TF_ID: regulatory motif matches from TRANSFAC
861	MIRNA_ID: miRNA targets from miRTarBase
862	CORUM_ID: protein complexes from CORUM
863	HPA_ID: tissue specificity from Human Protein Atlas
864	HP_ID: human disease phenotypes from Human Phenotype Ontology
865	

866 Description: description of the functional group

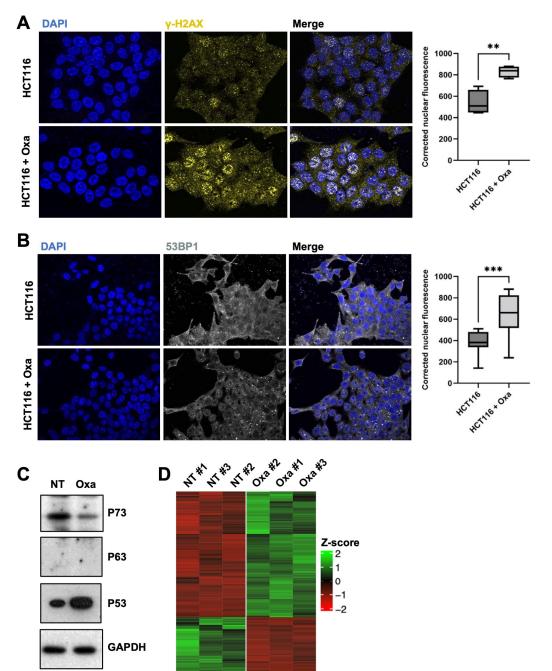
bioRxiv preprint doi: https://doi.org/10.1101/2023.03.17.533075; this version posted June 28, 2023. The copyright holder for this preprint (which was not certified by peer review) is the author/funder. All rights reserved. No reuse allowed without permission.

- 867 p.Val: p-value
- 868 FDR: false discovery rate
- 869 Genes: genes found in the intersection

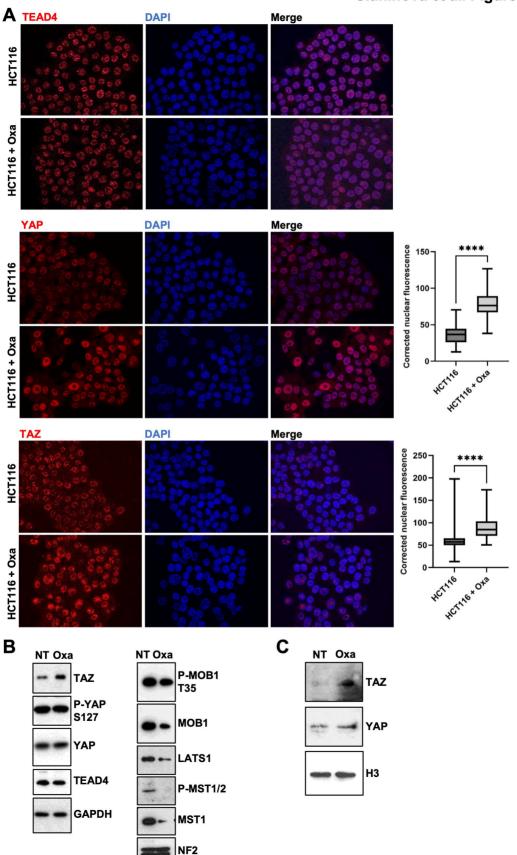
870

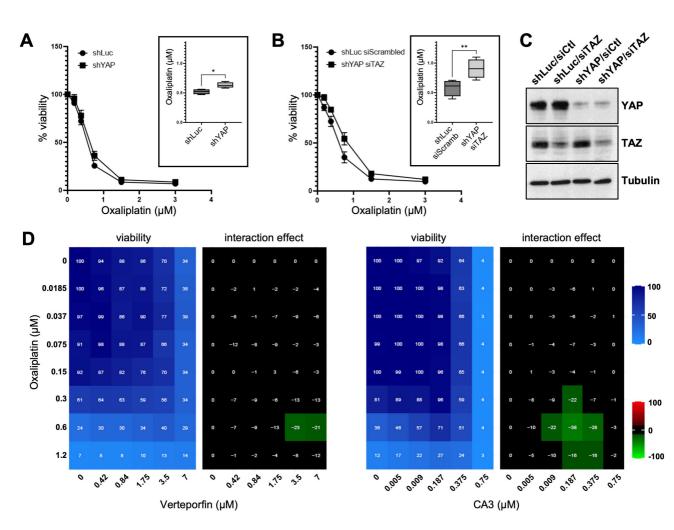
- 871 Supplemental Table 3. RNA-Seq statistics
- 872

Slaninova et al. Figure 1

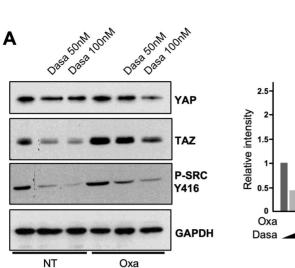


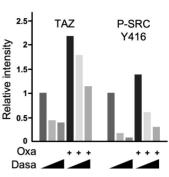
Slaninova et al. Figure 2



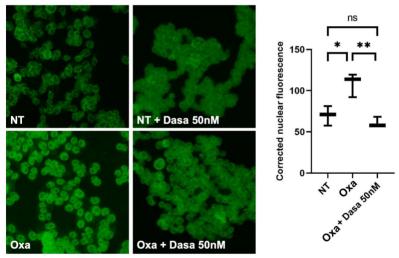


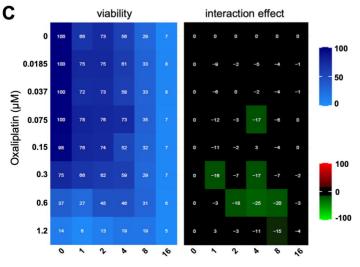
Slaninova et al. Figure 4











Dasatinib (µM)